

## Anomalous contrast and high sharpness of image of a sharp edge of a steel plate during radiography using microfocus bremsstrahlung of a new source based on an 18 MeV betatron

© M.M. Rychkov, V.V. Kaplin, V.A. Smolyanskiy

Tomsk Polytechnic University, Tomsk, Russia

E-mail: rychkov@tpu.ru

Received March 6, 2024

Revised June 21, 2024

Accepted July 4, 2024

A radiographic image of the sharp edge of a 0.4 mm thick steel plate, demonstrating the property of the microfocus bremsstrahlung of a new source based on an 18 MeV betatron to form a contrasting and sharp image of the plate edge tip, is presented. An anomaly in the form of a narrow light band along the positive image of the tip provides its contrast, which together with the high sharpness of the image due to the microfocus of the source makes it possible to determine the position of the tip with high accuracy. The light band effect is not observed when using 450 and 45 keV X-ray tubes with focus sizes of 400 and 80  $\mu\text{m}$ .

**Keywords:** betatron, electron beam, microfocus bremsstrahlung, radiography.

DOI: 10.61011/TPL.2024.11.59655.19914

Compact sources with a microfocus (smaller than 0.1 mm) spot and radiation energy in the megaelectronvolt range are needed in high-resolution radiography and tomography to increase the radiation thickness of the examined articles. Common high-energy microfocus X-ray tubes have the capacity to generate radiation with energies up to 450 keV only.

The first experiments with a new microfocus source based on the B-18 betatron with an electron energy of 18 MeV and narrow silicon (Si) and tantalum (Ta) internal targets, which provided a micrometer-level bremsstrahlung focus size, have been performed in [1,2]. It was demonstrated that this microfocus source is also efficient in producing high-contrast high-resolution magnified images of micro-objects such as pairs of thin wires of the Duplex image quality indicator [3]. When narrow (50 and 8  $\mu\text{m}$ ) Si targets were used, the involvement of phase contrast in the formation of images of edges of plastic and steel plates was also noted, revealing a fairly high spatial coherence of radiation. Magnified images [4] of gaps 10  $\mu\text{m}$  in width between steel blocks and tantalum foil 13  $\mu\text{m}$  in thickness, which were positioned behind steel barriers with a thickness of 40 and 55 mm, demonstrated a high sensitivity of their visualization with the use of the new microfocus radiation source with a narrow (13  $\mu\text{m}$ ) Ta target. A high sensitivity of detection of micro-objects in radiography of thick steel objects in experiments with the new betatron-based source was reported in [5]. Note that the concept of application of an internal target with a size smaller than the beam diameter of an orbit accelerator for reducing the radiation focus spot size has been proposed and examined for the first time in [6,7].

In the present study, we report the results of experiments demonstrating the contrast and sharpness of radiographic

images of a sharp edge of a steel plate that were obtained using radiation of X-ray tubes with accelerating voltages of 450 and 45 kV and the new microfocus radiation source based on the B-18 betatron. A distinct feature in the form of a narrow light band along the tip was noted in the positive image of the edge tip in experiments with the betatron-based microfocus source. This band is indicative of amplification of radiation within the mentioned narrow region, provides contrast of the image of the tip, and, combined with a high image sharpness attributable to the use of the microfocus source, allows one to determine its position with a high accuracy. No such band was observed in experiments with X-ray tubes with focus sizes of 400 and 80  $\mu\text{m}$ .

The diagram of the experiment with microfocus radiation of the B-18 betatron is shown in Fig. 1, *a*. A tantalum target with thickness  $t_m = 13 \mu\text{m}$ , height  $H = 10 \text{ mm}$ , and length  $T = 2.5 \text{ mm}$  along the electron beam was positioned vertically on a goniometer inside the betatron chamber at a radius shorter than the orbit radius of accelerated electrons and was oriented along the electron beam. An additional magnetic field produced by the dump winding at the end of the acceleration cycle reduced the orbit radius of electrons, and they hit the target. The generated bremsstrahlung with an energy up to 18 MeV has a linear focus with a vertical size equal to the electron beam diameter (1.4 mm) and a horizontal size depending on the horizontal angle of radiation emission from the target (see the inset in Fig. 1, *a*). Radiation left the chamber through a window covered with a lavsan film and was incident on a steel plate with thickness  $t_p = 0.4 \text{ mm}$ , a width of 18 mm, and a length of 10 cm positioned vertically (see the inset in Fig. 1, *a*) on an external goniometer at distance  $L_1 = 48 \text{ cm}$  from the target. An AGFA NDT D4 PbVacuPac X-ray film was mounted at distance  $L_2 = 116.5 \text{ cm}$  from the target. The

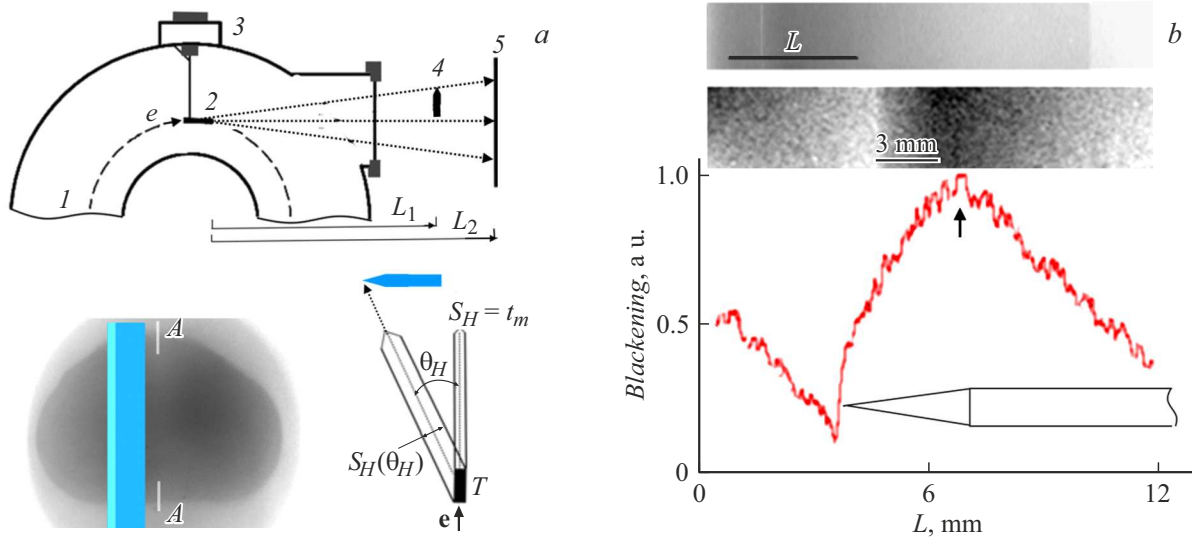


**Figure 1.** *a* — Diagram of the experiment. 1 — B-18 betatron chamber (top view); 2 — target oriented along the electron beam; 3 — goniometer; 4 — steel plate with a sharp edge; and 5 — X-ray film. The position of the plate with its left sharp edge in the radiation beam and the diagram illustrating the dependence of horizontal size  $S_H$  of the source on horizontal angle  $\theta_H$  of bremsstrahlung emission from the target are shown below. *b* — Densitogram of a magnified ( $M = 2.43$ ) positive image (see the upper inset) of the sharp edge of the steel plate. The lower inset shows an enlarged fragment of the image of the plate tip with a light mark (3 mm) that indicates the width of image of the sharp edge.

magnification factor of the image of the plate with a sharp edge  $l_p = 1.2$  mm in width positioned perpendicular to the axis of the radiation cone was  $M = L_2/L_1 = 2.43$ . Images were scanned for subsequent analysis.

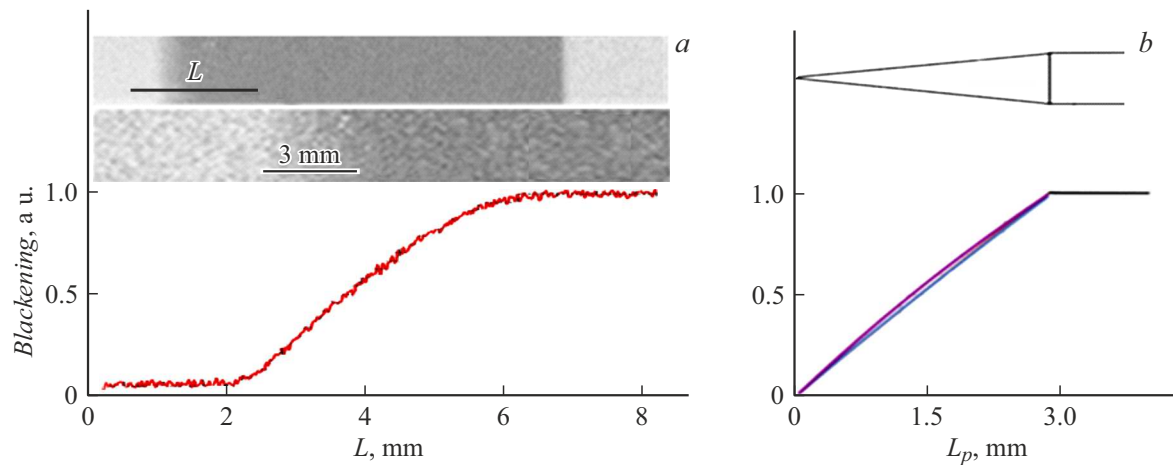
Figure 1, *b* presents the densitogram of a magnified ( $M = 2.43$ ) positive image of the sharp plate edge measured along line  $L$  in the image fragment shown in the upper inset. Projection  $A-A$  of the Ta target plane was located at distance  $t_e = 52$  mm from the image of the tip. Therefore [1], effective horizontal size  $S_H$  of the focus of the fraction of radiation incident on the left sharp edge is  $S_H(\theta_H) = t_m + T\theta_H = 127 \mu\text{m}$ , where  $\theta_H \approx t_e/L_2$  is the horizontal angle of radiation emission from the target. The contrast of image of the sharp edge is established by a narrow light band running along the edge tip. This anomaly in the form of a light band cannot be explained in terms of the formation of contrast due to radiation absorption. A change in radiation absorption in this region may induce only a gradual variation of blackening (i.e., a lack of edge contrast due to a gradual reduction of thickness  $t$  of the wedge-shaped edge to  $t = 0$ ). The presence of contrast and a high sharpness of the sharp plate edge image, which is specified by geometric blurring  $a_1 = S_H(M - 1) = 183 \mu\text{m}$  and intrinsic X-ray film blurring, attributable to the micro-focus nature of the source make it possible to establish the position of the tip with a fairly high accuracy. The maximum of the densitogram (marked with an arrow) corresponds to the origin of the sharp edge of the plate. The blackening increases within the interval from  $L = 12$  to 6.8 mm and at  $L < 3$  mm due to the fact that the plate is positioned on

the slope of the angular distribution of radiation (see the photographic image in Fig. 1, *a*).

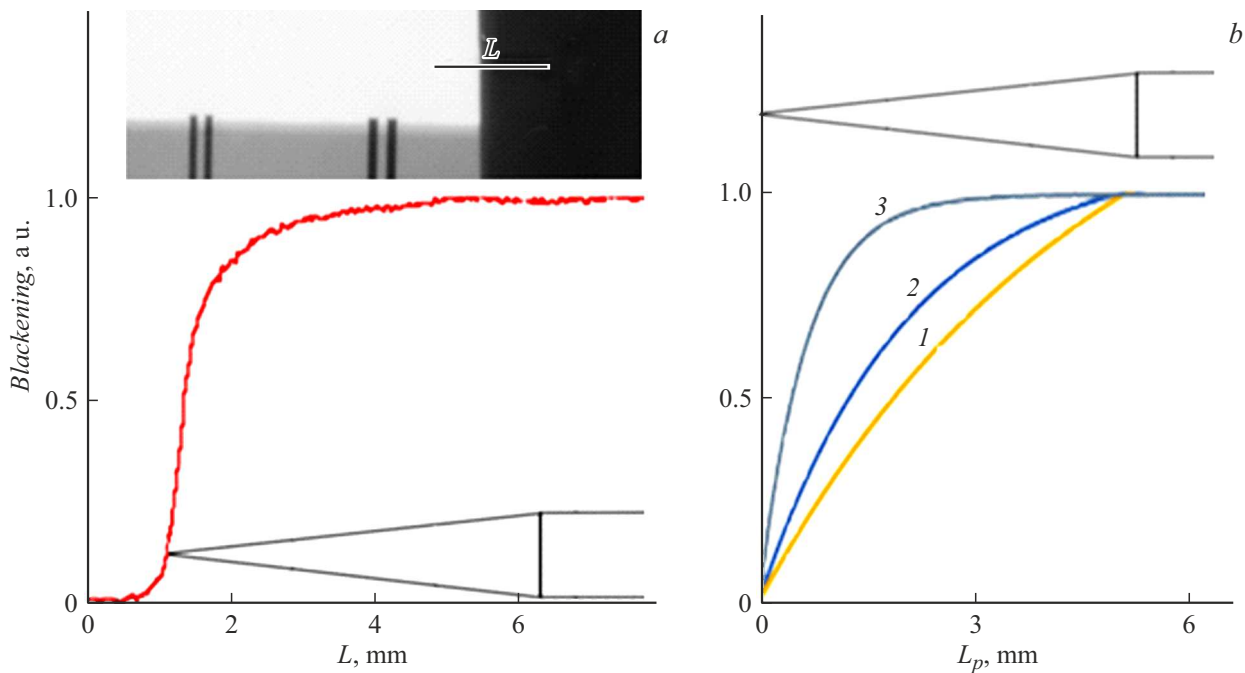
A gradual blackening reduction was observed in the image of the sharp edge of the plate obtained using the X-ray tube with a radiation energy up to 450 keV and a focus size of 0.4 mm. Figure 2, *a* presents the densitogram of a magnified ( $M = 2.3$ ) image of the sharp plate edge measured along line  $L$  in the image fragment shown in the upper inset. An additionally enlarged fragment of the image of the plate tip is shown in the lower inset. The densitogram reveals strong blurring of the plate tip image, which is attributable to the fairly large focus size of this source, and a gradual reduction in blackening with decreasing thickness of the wedge-shaped edge. A light band near the tip of the plate is not observed. Note that the variation of blackening on the slope of the densitogram is very close to the linear change in thickness of the wedge-shaped edge of the plate.

Figure 2, *b* shows the normalized profiles of blackening  $B(L_p)$  of the positive image of the plate tip for photon energies of 400, 200, and 100 keV calculated by approximate formula  $B(L_p) = N(1 - e^{-\mu k L_p})$  (where  $N$  is the normalization coefficient,  $\mu$  is the radiation attenuation coefficient, and  $k = t_p/Ml_p$ ), which is applicable at  $0 < L_p < Ml_p$ ; at  $L_p > Ml_p$ ,  $B(L_p) = 1$ . The profiles for energies of 400 and 200 keV match, while the dependence for 100 keV differs slightly from them. The calculated blackening profiles are very close to the blackening profile in the image densitogram.

Such data regarding the variation of thickness extracted from a radiographic image of an object are not always correct. To illustrate this, an experiment with X-ray tube



**Figure 2.** *a* — Densitogram of a magnified ( $M = 2.3$ ) positive image of the sharp edge of the steel plate obtained using the X-ray tube with a radiation energy up to 450 keV. The densitogram was measured along line  $L$  in the image fragment shown in the upper inset. The lower inset presents an enlarged fragment of the image of the plate tip. *b* — Calculated normalized blackening profiles for the image of the sharp edge of the plate at photon energies of 400, 200, and 100 keV.



**Figure 3.** *a* — Densitogram of a magnified ( $M = 4.3$ ) positive image of the sharp edge of the steel plate obtained using the X-ray tube with a radiation energy up to 45 keV. The densitogram was measured along line  $L$  in the plate image fragment shown in the inset. The four vertical lines in the inset are the images of two pairs of wires of the Duplex image quality indicator. *b* — Calculated normalized blackening profiles in the positive image of the sharp plate edge for photon energies of 40 (1), 30 (2), and 20 keV (3).

radiation with an energy up to 45 keV and a focus size of  $80\ \mu\text{m}$  was carried out. Figure 3, *a* presents the densitogram of a magnified ( $M = 4.3$ ) positive image of the sharp edge of the steel plate obtained using the X-ray tube with a radiation energy up to 45 keV. The densitogram was measured along line  $L$  in the image fragment shown in the inset. It follows from the densitogram that the image of the edge tip is blurred and the variation of blackening of the image of the sharp plate edge within its fragment

extending from  $L = 1$  to 6.2 mm differs greatly from the linear dependence of film blackening on thickness of this part of the plate.

Figure 3, *b* shows normalized blackening profiles  $B(L_p)$  calculated using the formula given above for the positive image of the sharp plate edge at photon energies of 40, 30, and 20 keV. It is evident that the blackening profile is shaped by radiation in the middle part of the spectrum. A source providing much higher radiation energy is needed

to characterize properly the thickness distribution along the edge. To perform a correct calculation, due consideration must be given to the radiation spectrum and the sensitivity of the X-ray film in different regions of this spectrum.

Note that an experiment with the X-ray tube with a radiation energy up to 45 keV was also performed for a different plate with thickness  $t_p = 0.1$  mm and sharp edge width  $l_p = 0.4$  mm. The densitogram of a magnified ( $M = 4.3$ ) positive image of the tip of this plate did also reveal that the variation of blackening within the corresponding region of the image differs from a linear dependence, but this difference is less pronounced than the one observed for the plate with thickness  $t_p = 0.4$  mm. This implies that a source with a higher radiation energy is needed to obtain such film blackening that reflects a linear change in thickness of the sharp plate part.

The presented results of the experiment with microfocus radiation of a betatron-based source demonstrated that the sharpness of image of a sharp edge of a steel plate is high due to the microfocus nature of the source. The effect of anomalous contrast (a narrow light band running along the edge tip in the image) cannot be explained within the concept of absorption contrast and warrants further study.

The probable directly proportional dependence of image blackening on radiation thickness of various sections of the examined object should also be studied in more detail for the purpose of determining the relation between the maximum radiation thickness of the object and the radiation energy of the source needed to obtain such a dependence that provides additional practically relevant data on the shape of various parts or defects of the composite object.

## Funding

This study was performed as part of the development program of the Tomsk Polytechnic University.

## Conflict of interest

The authors declare that they have no conflict of interest.

## References

- [1] M.M. Rychkov, V.V. Kaplin, K. Sukharnikov, I.K. Vaskovsky, *Exp. Theor. Phys. Lett.*, **103** (11), 723 (2016). DOI: 10.1134/S0021364016110114
- [2] M.M. Rychkov, V.V. Kaplin, E.I. Malikov, V.A. Smolyanskiy, V. Gentsel'man, I.K. Vas'kovskii, *J. Nondestruct. Eval.*, **37** (1), 13 (2018). DOI: 10.1007/s10921-018-0464-6
- [3] IE-NTD Ltd. [Electronic source]. <http://ie-ndt.co.uk/en4625astme2002duplexiqi.html>
- [4] M.M. Rychkov, V.V. Kaplin, V.A. Smolyanskiy, *J. Phys: Conf. Ser.*, **1327**, 012014 (2019). DOI: 10.1088/1742-6596/1327/1/012014
- [5] M.M. Rychkov, V.V. Kaplin, V.A. Smolyanskiy, *Tech. Phys. Lett.*, **49** (10), 37 (2023). DOI: 10.61011/TPL.2023.10.57055.19583.
- [6] H. Yamada, *Jpn. J. Appl. Phys.*, **35** (2A), L182 (1996). DOI: 10.1143/JJAP.35.L182
- [7] V.S. Pushin, V.L. Chakhlov, patent RU 2072643 (1997). <http://www.findpatent.ru/patent/207/2072643.html>

*Translated by D.Safin*